Lattice Thermal Conductivity of Impure Tin*

J. E. GUETHS,† P. L. GARBARINO, M. A. MITCHELL, P. G. KLEMENS, AND C. A. REYNOLDS
Physics Department and Institute of Materials Science, University of Connecticut, Storrs, Connecticut 06268
(Received 3 October 1968)

Measurements of the normal- and superconducting-state thermal conductivities (K^n and K^s) were made on seven cadmium-doped tin single crystals in the temperature range $1°K < T < 4°K$. Data from six specimens measured previously are also included in the analysis. Cadmium concentrations range from 0.04 to 0.97 at.%. The crystal orientations are grouped in the near perpendicular direction (direction of heat flow approximately perpendicular to the tin tetrad axis). The small fractional size of the normal-state lattice conductivity, K_g^n, precludes its direct determination from the normal-state data alone. However, the superconducting-state thermal conductivity is employed in a "universal curve" type of analysis, from which we deduce for K_g^n a $T^{2.21\pm0.04}$ dependence upon temperature and a $\rho_0^{-(0.21\pm0.04)}$ dependence upon residual resistivity. As the solid solubility limit is approached we find an additional lattice resistivity varying as $T^{-1.4}$ and increasing in magnitude with increasing impurity concentration. This is ascribed to phonon scattering by point defects and boundaries, using adjustable parameters describing the distortion about the impurity and the mean free path for boundary scattering. The best fit to our data yields values for the strain field size that are in good agreement with the x-ray data of Lee and Raynor. The apparent boundary scattering mean free path is much less than the sample diameter; this indicates large clusters of impurities in the alloy.

I. INTRODUCTION

THIS paper describes an experimental investigation into the lattice thermal conductivity of tin and dilute tin alloys at low temperatures. The thermal conductivity of tin has been the subject of several recent studies. These have centered on the gross effects of alloying on the thermal conductivity,[1] the effects of the superconducting-state energy-gap anisotropy on the thermal conductivity,[2,3] the normal-state lattice thermal conductivity for very impure tin specimens,[4,5] and the variation of the electronic thermal conductivity in both the superconducting and normal states with crystal direction.[6,7]

Previous experiments on specimens sufficiently impure so that the fractional lattice conductivities would be large employed polycrystalline samples. It is well known that the transport properties of tin are highly anisotropic.[2] Therefore, the present work has been done on alloy single crystals, eliminating ambiguity of interpretation resulting from possible net orientation effects in polycrystalline samples.

The normal- and superconducting-state thermal conductivities are conventionally expressed as the sum of two terms, one electronic (e) and one lattice (g), viz.,

$$K^n = K_e^n + K_g^n \quad \text{(normal state)}, \tag{1}$$

$$K^s = K_e^s + K_g^s \quad \text{(superconducting state)}. \tag{2}$$

We shall refer to the ratios K^s/K^n, K_e^s/K_e^n, and K_g^s/K_g^n, and denote them as R_T, R_e, and R_g, respectively.

The normal-state lattice conductivity of very impure tin alloys in the temperature interval 1–5°K has been investigated by Hulm[4] and Garfinkel and Lindenfeld.[5] They found that K_g^n is a smaller fraction of K^n in tin than is normal for most alloy systems,[8] and, as a consequence, heavy doping is necessary even to make the fractional size of K_g^n only a few percent. In both of these investigations, K_g^n was obtained directly from the normal-state data alone. In our recent investigations into the effects of alloying on the thermal conductivity of tin[1] and into the energy gap anisotropy of tin[2] we noticed that, for our most impure specimens, the superconducting-state data could be used along with the "universal curve" formalism of Lindenfeld and Pennebaker[9] to draw quantitative conclusions as to the behavior of K_g^n. We have thus undertaken the present investigation into the lattice thermal conductivity of tin, and have chosen the characteristics (orientation, impurity concentration) of the specimens to be measured with this objective specifically in mind.

The theoretical ratio of superconducting to normal-state lattice conductivity R_g was calculated as a function of reduced temperature $t = T/T_c$ for superconductors in general by Bardeen, Rickayzen, and Tewordt[10] for the case when phonon-conduction electron scattering dominates both K_g^s and K_g^n. Klemens and Tewordt[11] extended the calculation to include point-defect scattering of phonons by impurities of different mass, and found that R_g is expected to be a function of

* Supported by the U. S. Air Force Office of Scientific Research Grant No. AF-AFOSR-474-67 and Office of Naval Research under Contract No. NONR 2967(00).
† Present address: Wisconsin State University, Oshkosh, Wisc.
[1] G. J. Pearson, C. W. Ulbrich, J. E. Gueths, M. A. Mitchell, and C. A. Reynolds, Phys. Rev. **154**, 329 (1967).
[2] J. E. Gueths, N. N. Clark, D. Markowitz, F. V. Burckbuchler, and C. A. Reynolds, Phys. Rev. **163**, 364 (1967).
[3] C. W. Ulbrich, D. Markowitz, R. H. Bartram, and C. A. Reynolds, Phys. Rev. **154**, 338 (1967); F. V. Burckbuchler, D. Markowitz, and C. A. Reynolds, *ibid.* **175**, 543 (1968).
[4] J. K. Hulm, Proc. Roy. Soc. (London) **A204**, 98 (1950).
[5] M. Garfinkel and P. Lindenfeld, Phys. Rev. **110**, 883 (1958).
[6] A. M. Gûenault, Proc. Roy. Soc. (London) **A262**, 420 (1961).
[7] N. V. Zavaritskii, Zh. Eksperim. i Teor. Fiz. **39**, 1571 (1960) [English transl.: Soviet Phys.—JETP **12**, 1093 (1961)].
[8] P. Lindenfeld, in *Proceedings of the Seventh International Conference on Low-Temperature Physics, 1960*, edited by G. M. Graham and A. C. Hollis Hallet (University of Toronto Press, Toronto, 1961), p. 279.
[9] P. Lindenfeld and W. B. Pennebaker, Phys. Rev. **127**, 1881 (1962).
[10] J. Bardeen, G. Rickayzen, and L. Tewordt, Phys. Rev. **113**, 982 (1959).
[11] P. G. Klemens and L. Tewordt, Rev. Mod. Phys. **36**, 118 (1964).

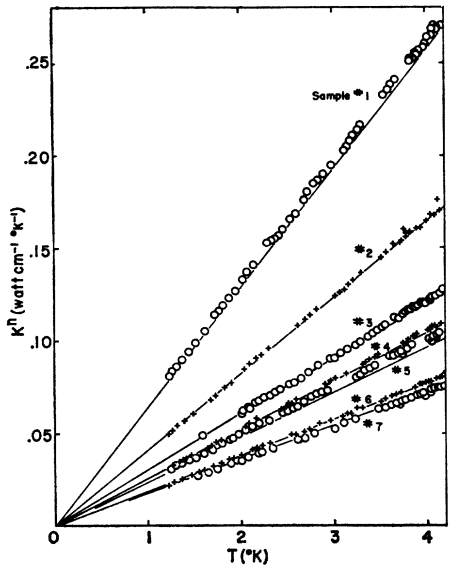

FIG. 1. K^n versus T for specimens measured in this work. The solid lines are calculated from the Wiedemann-Franz law, $K_e^n = L_0 T/\rho_0$.

point-defect content, which is proportional to ρ_0 when the density of point defects is large. Experimental determinations of R_g are few; our two previously mentioned papers treat this ratio only peripherally. One of our objectives is thus to experimentally determine the dependence of R_g on t in the case when phonon-conduction electron scattering is the primary contributor to the superconducting and normal-state lattice thermal resistivity.

The scattering of phonons either by point defects or by imperfections associated with impurities can become significant as impurity concentrations increase.[12–14] Since well below the transition temperature few electronic excitations are present to scatter phonons, any additional phonon scattering should become evident in the K^s-versus-t data. We expect that K_g^s will be abnormally depressed if such scattering is present in significant amounts.

In two recent investigations,[2,15] we have obtained information on the superconducting properties and the electronic thermal conductivity of tin single crystals containing cadmium. We have again chosen cadmium as the impurity so that data on our most impure previously measured specimens might be incorporated in the analysis. Single crystals having orientations in the near-perpendicular (cylindrical-specimen axis perpendicular to tetrad axis) direction were again selected so that any orientation effect will to a first approximation be the same for all specimens and can therefore be neglected. Impurity concentrations ranging up to the solid solubility limit of cadmium in tin ($\approx 1\%$) were introduced so as to produce the maximum relative magnitude of K_g^s/K^s and K_g^n/K^n.

In summation, the specific goals of this work are

(i) to determine the size of K_g^n in tin and its dependence on ρ_0 and T using the universal curve formalism of Lindenfeld and Pennebaker;

(ii) to determine whether the dependence of R_g on t is adequately described by the theory for the case of phonon scattering by conduction electrons;

(iii) to determine whether additional phonon scattering processes associated with the cadmium impurities can be observed in K_g^s as the solubility limit is approached.

TABLE I. Summary of sample characteristics.

Sample No.	ρ_0 ($\mu\Omega$ cm)	$1/G\times 100$ (at.%)[a]	θ[b] (deg)	L (mm)	S^2
1a	0.0675	0.042	59½	...	...
2a	0.0704	0.049	75	...	...
3a	0.0894	0.063	78½	...	...
4a	0.173	0.122	80½	...	...
5a	0.357	0.251	78½	...	...
1	0.381	0.274	57½	...	...
6a	0.460	0.32	77	...	...
2	0.595	0.43	68½	...	...
3	0.808	0.58	77	0.30	0.1
4	0.94	0.68	72½	0.60	0.02
5	1.01_5	0.73	79½	0.135	0.1
6	1.27_5	0.92	79	0.09	0.06
7	1.35	0.97	76½	0.08	0.1

[a] Calculated using $\rho_0 = 1.39$ $\mu\Omega$ cm/at.% (Ref. 15).
[b] Angle between the tetrad axis and the cylindrical axis of the specimen.

II. EXPERIMENTAL DETAILS

The cadmium-tin solid solution crystals were prepared and orientations determined in a manner previously described,[15] with two exceptions:

(i) The molds in which the crystals measured in this work were grown were 3-mm precision-bore Pyrex tubing. Our previous measurements were on 2-mm diam crystals. The larger cross-sectional area is desirable for the more impure (lower-thermal conductivity) specimens.

(ii) Measurements of ρ_0 as a function of annealing time (at 200°C) on a 0.2% Cd crystal showed changes even after 72 h, the annealing period in the previous work. We therefore annealed the specimens in this work for ≈ 300 h at 200°C. We consider this to be sufficient for specimens of impurity concentration not near the solubility limit. However, for our most impure specimens ρ_0 continued to decrease by about 2–3% over a period of 3–6 weeks at room temperature, suggesting that a slow rearrangement of impurities was continuing.

The thermal conductivity apparatus was identical to that shown in Fig. 1(b) of Ref. 2, and the experimental procedure was the same as that described there. The present specimens were sufficiently impure so that

[12] P. G. Klemens, Solid State Phys. 7, 1 (1958).
[13] K. Mendelssohn and H. M. Rosenberg, Solid State Phys. 12, 223 (1961).
[14] H. M. Rosenberg, *Low Temperature Solid State Physics* (Oxford University Press, London, 1963), p. 59.
[15] J. E. Gueths, C. A. Reynolds, and M. A. Mitchell, Phys. Rev. 150, 346 (1966).

magnetoresistance corrections were unnecessary, but small corrections were made to the data for heat generated in the current leads to the heater and heat lost by conduction along the leads from the hot thermometer and heater.

A microvolt potentiometer was used to determine electrical resistivities on sections of crystal symmetrically located with respect to the thermometer clamps (separation ≈ 6.5 cm). Measurements were made at 4.2°K and are reported as ρ_0, since the temperature-dependent resistivity for samples having impurity concentrations typical in this work is negligible.

Resistivity determinations at 77 and 273°K were consistent with the orientation and impurity concentration dependent values determined in a previous work.[15] The characteristics of the samples included in this work are given in Table I. Samples 1–7 are those measured in this work. Samples 1a–6a are samples 7–12, respectively, previously reported.[2]

III. RESULTS AND DISCUSSION

A. Normal-State Thermal Conductivity

The thermal conductivity in the normal state for all specimens measured in this work is plotted versus temperature in Fig. 1. The solid lines associated with each set of data represent the normal-state thermal-conductivity curve the data would be expected to follow if the conductivity were totally electronic and the Wiedemann-Franz law were obeyed ($K_e^n = L_0 T/\rho_0$, where $L_0 = 2.45\times10^{-8}$ $W\ \Omega\ °K^{-2}$). Within experimental error, the data satisfy the Wiedemann-Franz law. In fact, only two specimens (Nos. 1 and 5) exhibit slight variations from the solid line. In these cases, plots of K^n/T versus T exhibited zero slope. We conclude that a significant lattice conductivity is not evident in Fig. 1.

This result is somewhat disturbing, as we anticipate that our most impure specimens (Nos. 6 and 7) should exhibit fractional lattice conductivities of 4% at $T = 3.5$°K *if* the normal-state lattice conductivity follows the universal curve of Lindenfeld and Pennebaker[9] scaled to tin. (We shall later use the superconducting-state thermal-conductivity data to show that this, in fact, is the case.) Small geometrical uncertainties in the thermal conductivity measurement and errors in the ρ_0 determination have apparently thwarted our efforts to resolve K_g^n in the normal-state data alone.

B. Superconducting-State Thermal Conductivity

We indirectly exhibit the superconducting-state thermal conductivity as a plot of R_T versus $t = T/T_c$ in Fig. 2. The data were obtained by dividing the K^s data by the values of K^n lying on a smooth curve drawn through the K^n-versus-T data. Superconducting-transition temperatures (T_c) were obtained using the known T_c-versus-ρ_0 dependence for cadmium-doped tin single crystals.[15] The advantages of using this form of the superconducting-state thermal-conductivity data for analytical purposes has been discussed previously.[1] The effects of geometrical uncertainties rooted in the finite width of the thermometer mounts and systematic errors of various types are minimized in the ratio R_T. We will attempt to employ the variation of R_T with ρ_0, at constant T, to investigate K_g^n and R_g.

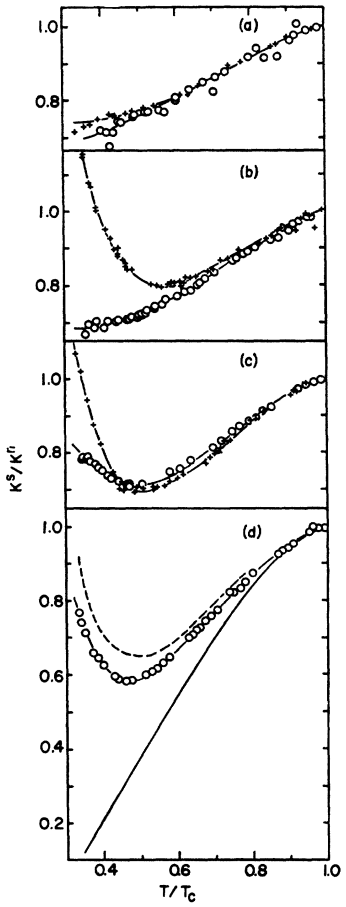

FIG. 2. $R_T = K^s/K^n$ versus t for all specimens measured in this work. (a) (○), sample No. 7, $\rho_0 = 1.35$. (+), sample No. 6, $\rho_0 = 1.27$. (b) (○), sample No. 5, $\rho_0 = 1.01$. (+), sample No. 4, $\rho_0 = 0.94$. (c) (○), sample No. 3, $\rho_0 = 0.81$. (+), sample No. 2, $\rho_0 = 0.595$. (d) (○), sample No. 1, $\rho_0 = 0.38$. (— — — —), sample No. 6a, $\rho_0 = 0.45$, from a previous work (Ref. 2). (———), the $R_e = K_e^s/K_e^n$ curve using $2\Delta(0)/k_B T_c = 3.7$ in a calculation of the Kadanoff and Martin type.

We obtain the lattice conductivity in the superconducting state from

$$K_g^s/K^n = K^s/K^n - K_e^s/K^n = R_T - R_e, \qquad (3)$$

and, since for all our specimens $K_g^n/K^n \leqq 0.04$, we can approximate $K^n = K_e^n$ in the denominator. In particular for K_e^s/K^n we can use the ratio $R_e = K_e^s/K_e^n$, given by the theory of Kadanoff and Martin.[16]

[16] Leo P. Kadanoff and Paul C. Martin, Phys. Rev. 124, 670 (1961).

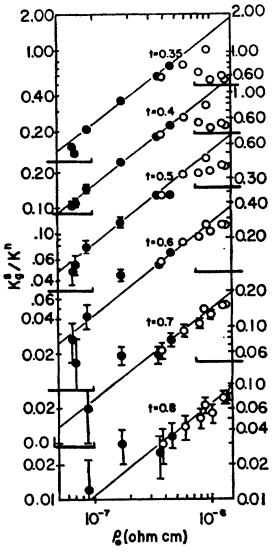

FIG. 3. Plots of K_g^s/K^n versus residual electrical resistivity ρ_0 at six values of reduced temperature. Estimated uncertainties due to scatter in K^s and K^n are indicated by the error bars. (●), samples 1a–6a from a previous work (Ref. 2). (○), all samples measured in this work. The solid lines drawn through each set of data are parallel. The abnormal depression of K_g^s at larger ρ_0 and lower t indicates that another phonon-scattering mechanism is contributing to W_g^s.

To obtain the values of K_g^s/K^n we have had to assume the variation of R_e with temperature and ρ_0. We had previously demonstrated[2] that the effect on R_e of the anisotropy of the energy gap essentially disappears in the case of tin when ρ_0 exceeds 10^{-7} ohm cm. With continued introduction of impurities, one reasonably expects only small effects on the ratio R_e, and that it should vary only slowly with concentration. It was also shown previously that $R_e(t)$ is well approximated by the theoretical results of Kadanoff and Martin[16] using an isotropic energy gap of $2\Delta(0)/k_BT=3.7$. In the present work it is assumed that this functional form of $R_e(t)$, shown as the bottom line in Fig. 2(d), applies to all specimens. Values of K_g^s/K^n thus obtained are plotted in Fig. 3.

We also assume that K_g^n is given *in form* by the universal curve of Lindenfeld and Pennebaker,[9] so that K_g^n as functions of ρ_0 and T is given by

$$K_g^n/\rho_0 T = C(T/\rho_0)^{n-1}, \tag{4}$$

where C and n are constants to be determined experimentally. Taking logarithms, writing $K_g^n = K_g^s/R_g$, using (3) and using the Wiedemann-Franz law for K_e^n, we obtain

$$\ln(K^s/K^n - K_e^s/K_e^n) = \ln(R_T - R_e) = \ln(CR_g t^{n-1} T_c^{n-1}/L_0) + (3-n)\ln\rho_0. \tag{5}$$

If we now take the ratio R_g to be independent of ρ_0, we can determine the index n from the slope of the logarithmic plot of $(R_T - R_e)$ against ρ_0 at constant temperature. This assumption is almost certainly valid, provided phonon scattering by defects can be neglected in the superconducting state. We shall see later that this is not entirely true, particularly at lowest temperatures (where phonon-electron scattering in the superconducting state is smallest) and for the highest impurity concentrations (where either the solute atoms or imperfections genetically related to them add to the phonon scattering). A second requirement is, of course, that K_g^n is not affected by these other scattering mechanisms; however, K_g^n will always be less affected than K_g^s. These plots will also give us $\ln(CR_g(t))$, and we can obtain C separately from the requirement that $R_g = 1$ at $t = 1$.

Thus, Fig. 3 is a plot of $\ln(K_g^s/K^n)$, or the left-hand side of (5), against $\ln(\rho_0)$ at six reduced temperatures for the seven specimens measured in the present work, and the six most impure crystals of our previous work.[2] The data are seen to fall on straight lines, except for marked deviations at lower temperature and higher ρ_0. These deviations are interpreted as being due to a variation of R_g with ρ_0 via an additional phonon-scattering mechanism, and will be discussed below. The solid lines drawn through each set of data were constrained to be parallel and to fit the data at each reduced temperature in the regions of lower ρ_0. The line slope $(3-n)$ in Eq. (5) is determined to be 0.79 ± 0.04, so that K_g^n varies as $T^{2.21\pm0.04}$ in regions of high-temperature and low-impurity concentration.

The ordinates of the straight lines in Fig. 3 are a measure of the product $CR_g(t)$ for phonon scattering by electrons. These values are plotted in Fig. 4 as a function of reduced temperature t. These may be compared with the theoretical $R_g(t)$ curve of Klemens and Tewordt[11] in the case when there is no point-defect scattering. On a logarithmic scale the theoretical curve, i.e., the solid curve of Fig. 4, can be moved vertically to fit the experimental points; each experimental point is compounded from the straight line best fit of Fig. 3. If we now require that $R_g = 1$ at $t = 1$, we can determine

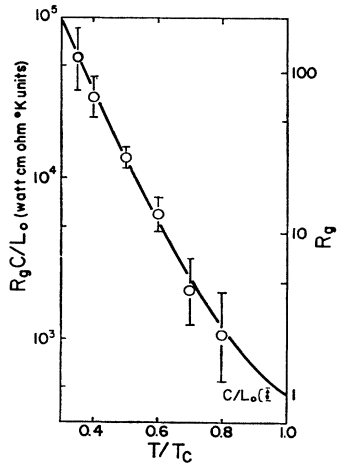

FIG. 4. Values of R_gC/L_0 obtained from the solid lines in Fig. 3 plotted versus reduced temperature t. The error bars represent uncertainties in the locations of these lines due to data uncertainties. The solid line is an R_g versus t plot taken from Fig. 1 of Ref. 11 which has been adjusted vertically for the best fit to the data (see the scale on the right side of the figure). The uncertainty in the determination of $C/L_0 = (4.6\pm0.4)\times10^2$ is represented in the lower right-hand corner of the figure. The shape of the theoretical R_g-versus-t curve is well represented by our data.

C and $R_g(t)$ separately. It is seen that the experimental R_gC/L_0 curve as a function of t agrees quite well with the theoretical $R_g(t)$ curve.

In this way we obtain a value of $C=(1.13\pm0.10)\times10^{-5}$ in the W Ω cm °K system of units, so that we can fit the normal-state lattice thermal conductivity to the form given by (4) as follows:

$$K_g{}^n=\frac{(1.13\pm0.10)\times10^{-5}T^{2.21\pm0.04}}{\rho_0{}^{0.21\pm0.04}}, \qquad (6)$$

where $K_g{}^n$ has units of W/cm °K, ρ_0 is in Ω cm, and T is in °K. Figure 5[17] represents a "universal curve" scaled to tin, on which this result is shown as the dashed line. The solid line represents the result of Lindenfeld and Pennebaker[9] for the case when the longitudinal and transverse modes interact with the electrons nearly independently of each other.

C. Additional Phonon Scattering

We now direct our attention to the additional phonon thermal resistivity apparently present in our more impure specimens, as suggested by the data in Fig. 3. Although the additive resistance approximation may be a poor one, we have little choice but to use it in the first instance, as we do not have any way of *a priori* determining the scattering mechanism(s) leading to the increased phonon resistivity. Thus, we write

$$W_g{}^s=W_g{}^s(\text{p-e})+W_g{}^s(x), \qquad (7)$$

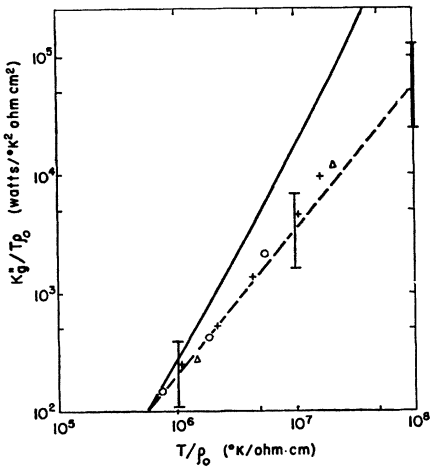

FIG. 5. Comparison of our expression for the normal-state lattice conductivity of tin with the universal curve scaled to tin. The solid line represents the theoretical curve of Lindenfeld and Pennebaker for the case in which the longitudinal and transverse phonon modes simply sum. The ○'s, +'s, and △'s are representative points taken from the curves for silver (Ref. 17), copper (Ref. 10), and indium (Ref. 19) scaled to the tin curve. The dashed line is a plot resulting from our expression, Eq. (9), for the lattice conductivity. The error bars represent the uncertainty in the location of the line due to the uncertainties in the constants.

[17] M. H. Jericho, Phil. Trans. Roy. Soc. London **A257**, 385 (1965).

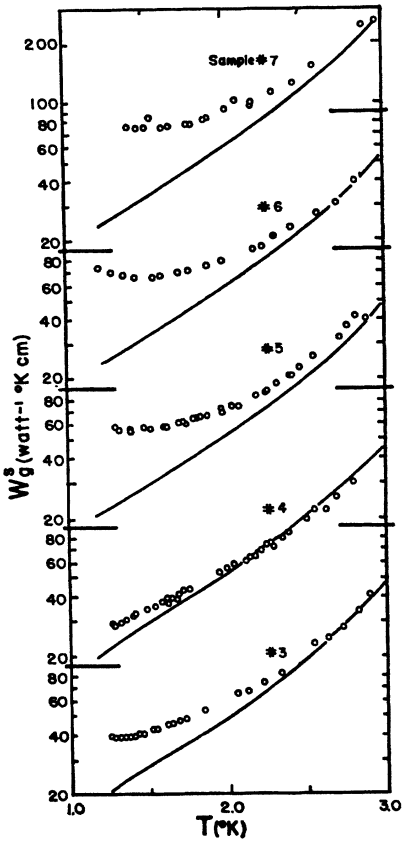

FIG. 6. Plots of $W_g{}^s$ versus T for the five most impure specimens in this work. Impurity concentration increases from bottom to top. The solid lines represent values to be expected if the only significant lattice thermal-resistivity mechanism is phonon-conduction electron scattering. The additional lattice thermal resistivity is most evident at the lowest temperatures, where the number of conduction electrons available to scatter has been reduced via condensation into the super state. We note that sample No. 4 does not exhibit as much additional phonon scattering as might be expected. This indicates that the additional term in $W_g{}^s$ may not be a simple function of impurity concentration or that sample No. 4 is unusual in some manner.

where $W_g{}^s=1/K_g{}^s$ is the total superconducting-state lattice thermal resistivity, and $W_g{}^s(\text{p-e})$ and $W_g{}^s(x)$ are the resistivity terms appropriate to phonon scattering by conduction electrons and the unknown mechanism, respectively.

The straight lines in Fig. 3 are taken to represent $W^n/W_g{}^s(\text{p-e})$ as a function of ρ_0 at the various values of t. Using the ρ_0 values and the curves for our five most impure specimens (where another scattering mechanism is present as indicated by significant deviations from the straight lines in Fig. 3), along with the measured K^n values, we construct $W_g{}^s(\text{p-e})$ as a function of t for each of these specimens. These are shown as the solid lines in Fig. 6. The $K_e{}^s/K_e{}^n$ curve for $2\Delta(0)/k_BT_c=3.7$ (bottom solid line in Fig. 2) is then subtracted from the K^s/K^n data in Fig. 2 to obtain $K_g{}^s/K^n$-versus-t data for each specimen. $W_g{}^s$ values were then obtained by employing smooth curves drawn

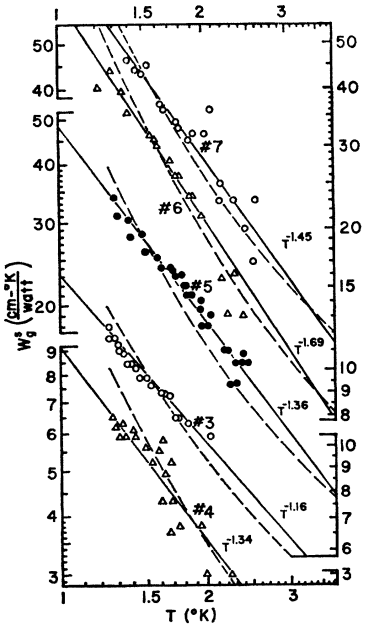

FIG. 7. $W_g^s(x)$, the difference between the data and solid line of Fig. 6, plotted versus temperature. The average slope of the lines drawn through the data is ≈ 1.4, indicating that $W_g^s(x) \propto T^{-1.4}$. In general, we see that $W_g^s(x)$ decreases with decreasing impurity concentration. The dashed lines are the point-defect–boundary scattering theory fitted to each sample with L and S^2 values given in Table I.

through the K^n data in Fig. 1. These data are also shown in Fig. 6.

We note that all five of these specimens exhibit some degree of additional phonon scattering of an unknown nature. The difference between the W_g^s data and the W_g^s(p-e) solid lines is taken to represent $W_g^s(x)$. This is subsequently plotted versus T on full logarithmic paper to establish the temperature dependence of $W_g^s(x)$ if one exists. This is shown in Fig. 7. It is seen that $W_g^s(x)$ follows a similar simple temperature dependence for all five specimens [i.e., $W_g^s(x)=AT^n$, where $n=-1.4$]. Although the slopes of the individual lines vary slightly about this value, it must be remembered that we are dealing with very small differences and a rather limited temperature interval. Further, systematic error could be introduced into Fig. 7 by the following: (i) A systematic variation of R_e with impurity concentration (although we expect this to be small, it could enter into the data in Fig. 7 to a significant degree). (ii) The failure of the additive-resistance approximation. (iii) The failure of the assumption that R_g is approximately independent of impurity concentration in the range of lower ρ_0, and higher temperatures.

TABLE II. α versus $I(\alpha)$.

α	$I(\alpha)$	α	$I(\alpha)$
10^{-6}	25.92	5×10^{-2}	10.65
10^{-5}	25.59	10^{-2}	8.202
10^{-4}	23.49	5×10^{-1}	3.935
6×10^{-4}	18.75	10^{-1}	2.734
10^{-3}	16.90	5	0.2443

A lattice thermal resistivity $W_g \propto T^n$ with n between -1 and -2 would indicate scattering of phonons by dislocations or by stacking faults.[12] It should be remembered, however, that n has been determined over a limited temperature range only, and may be the result of two different imperfections acting in combination.

Since boundaries and isolated point defects certainly scatter phonons in these specimens, it is tempting to try to explain W_g^s in terms of these two scattering mechanisms. One can write

$$1/W_g^s = K_g = \tfrac{1}{3}\sum_j \int S_j(\omega) v_j \Lambda(\omega) d\omega, \tag{8}$$

where $S_j(\omega)d\omega$ is the specific heat per unit volume due to phonons of frequency ω, the sum is over polarizations j, v_j is the phonon velocity and $\Lambda(\omega)$ the phonon mean free path. For boundary scattering and point-defect scattering

$$1/\Lambda = 1/\Lambda_B + 1/\Lambda_p, \tag{9}$$

where $\Lambda_B = L$ is a frequency-independent mean free path which, in a perfect crystal, should be comparable to the specimen diameter, while the point-defect mean free path is given by[12,18]

$$1/\Lambda_p = (3a^3/\pi v^4 G) S^2 \omega^4. \tag{10}$$

In (10), a^3 is the atomic volume and G the reciprocal of the defect concentration (per atom). The parameter S^2 describes the strength of the scattering.

Using a Debye expression for the specific heat and approximating v with the transverse sound velocity, we obtain, for K_g,

$$K_g = (4\pi L k_B^4/v^2h^3) T^3 I(\alpha) = 0.00562 L T^3 I(\alpha), \tag{11}$$

where

$$I(\alpha) = \int_0^\infty \frac{x^4 e^x dx}{(e^x-1)^2(1+\alpha x^4)} \tag{12}$$

and L is expressed in mm, and T is expressed in °K. The parameter α is given by

$$\alpha = [3(2\pi)^4 k_B^4 a^3 L T^4]/\pi v^4 h^4 G = 3.92 (S^2/G) L T^4. \tag{13}$$

The definite integral $I(\alpha)$ has been evaluated for various values of α on the University of Connecticut IBM 360 computer, and some values are given in Table II.

By adjusting L and S^2 for each sample it was possible to fit (11) to the data. The values of L and S^2 required

[18] P. G. Klemens, Proc. Phys. Soc. (London) A68, 113 (1955).

TABLE III. Various contributions to the thermal conductivity of sample No. 7.[a]

T (°K)	K^n	K^s	K_e^n [b]	K_e^s [c]	K_g^n [d]	K_g^s [e]	K_g^s(p-e)[f]	$K_g^s(x)$[g]
1.49	0.0270	0.0192	0.0270	0.00552	0.00046	0.0133	0.0302	0.0233
2.60	0.0471	0.0405	0.0470	0.0334	0.0016	0.00648	0.00735	0.0513
3.72	0.0666	0.0666	0.0631	0.0631	0.00357			

[a] All thermal conductivity values are given in units of W/cm °K. Geometrical uncertainties limit the accuracy of the superconducting- and normal-state thermal conductivities K^s and K^n, respectively, taken from the raw data to 2%.

[b] The normal-state electronic conductivity calculated from $K_e^n = TL_0/\rho_0$. ρ_0 is known to ±3% for samples near the solubility limit.

[c] The superconducting-state electronic conductivity as found from $K_e^n R_s$. For R_s the curve of Kadanoff and Martin (Ref. 16) with $2\Delta(0)/k_B T_c = 3.7$ was used.

[d] The normal-state lattice conductivity as calculated from the results of the "universal curve" analysis [Eq. (6)]. The small fractional size of K_g^n and experimental uncertainties preclude direct evaluation from $K^n - K_e^n$.

[e] The superconducting-state lattice thermal conductivity equal to $K^s - K_e^s$. Found from a smooth curve drawn through the data points of Fig. 6, $(K_g^s = 1/W_g^s)$.

[f] K_g^s as limited by phonon-electron scattering. Based on the "universal curve" analysis. Found from the family of solid lines in Fig. 3 as plotted versus temperature in Fig. 6.

[g] K_g^s as limited by the "extra" phonon-scattering mechanism equal to $[1/K_g^s - 1/K_g^s(\text{p-e})]^{-1}$. Found from the straight line of best fit (solid line) to the data points in Fig. 7.

to do so are given in Table I. The curves of W_g^s thus obtained are given in Fig. 7 as dashed lines.

The mass difference between Cd and Sn is too small to account for the point-defect scattering. Theoretically, $S^2 = (1/12)(\Delta M/M)^2$, and in this case one would obtain $S^2 = 3\times10^{-4}$. The observed values seem grouped around 1×10^{-1} or a little less. This scattering should probably be ascribed to the anharmonic scattering of the distortional strain field about each impurity. This mechanism should yield a value[19] for S^2 of

$$S^2 = 3\gamma^2(\Delta R/R)^2, \tag{14}$$

where γ, the Grüneisen constant, should be about 2, and $\Delta R/R$ is the fractional radial distortion of the impurity. To fit the data, one would require $\Delta R/R \approx 9\times10^{-2}$. From the change of lattice spacing of Sn-Cd alloys with increasing Cd concentrations,[20] it appears that $\Delta R/R \approx 4\times10^{-2}$, so that the point-defect scattering needed to fit the data appears to be of reasonable magnitude.

The boundary mean free path required to fit the data is much smaller than the external diameter of the specimens. Since the specimens were single crystals, and since the scattering by small-angle grain boundaries is very weak, this scattering cannot be due to boundaries. It is suggested here that the frequency-independent scattering mechanism limiting Λ_B is due to precipitates of cadmium in the alloy matrix. In order for scattering to be frequency independent, the diameter of the precipitates must be at least 100 atom sites in diameter.[12] If a precipitate contains n atoms, and there are N precipitates per unit volume, and if the scattering cross section is equated to the geometrical cross section,

$$\frac{1}{\Lambda} \approx N a^2 n^{2/3},$$

while the fraction of cadmium atoms thus involved in precipitation is $1/N\ a^3 n$. Taking $n \approx 10^6$, so that the precipitate is large enough to scatter independently of frequency, a mean free path of 0.1 mm requires precipitate concentration of the order of $N \approx 10^{11}$ per cm^2. This would require 10^{17} atoms/cm^3 to be in precipitates. The total impurity concentration is of the order of 10^{20} per cm^3, only a small amount of precipitation is therefore needed to account for the small mean free path. As we are dealing with alloys near the limit of solid solubility, and since it has been observed that ρ_0 decreases slowly on annealing, this precipitation is quite possible.

IV. SUMMARY

We have utilized the superconducting-state thermal conductivity to determine an expression for the normal-state lattice thermal conductivity of impure tin in terms of ρ_0 and T for the case when the lattice conductivity is limited by phonon-conduction electron scattering. This expression is qualitatively and quantitatively consistent with the universal curve formalism for dilute alloy normal-state lattice conductivities proposed by Lindenfeld and Pennebaker. The ratio of superconducting to normal-state lattice thermal conductivity as calculated by Klemens and Tewordt for scattering of phonons primarily by electrons is supported by our experimental results. At low temperatures and impurity concentrations approaching the solid solubility limit, another lattice thermal-resistivity term was observed in the superconducting-state data and subsequently isolated. The magnitude of this additional lattice resistivity was found to increase with increasing impurity concentration.

A theoretical expression for the lattice thermal conductivity limited by point-defect and frequency-independent or "boundary" scattering, which contained two adjustable parameters S^2 and L, could be fitted to the experimentally determined additional resistance. The parameter S^2, a measure of the effectiveness of point-defect scattering, was found to have values of similar magnitude to those that would be deduced from the fractional change of lattice parameter with increasing impurity content. The parameter L, a measure of

[19] P. G. Klemens, Phys. Rev. **169**, 229 (1968).

[20] J. A. Lee and G. V. Raynor, Proc. Phys. Soc. (London) **B67**, 737 (1954).

the constant phonon mean free path at very low frequencies, was found to have values much less than the specimen diameter. This could be due to a precipitation of cadmium impurity in the alloy matrix.

Finally, in order that the reader might easily obtain a feel for the relative magnitudes of the effects discussed, we summarize the results by listing in Table III the various conductivities discussed for the most impure sample, No. 7. It is evident from the last two columns that the additional phonon scattering mechanism evident in our data is of quite comparable size to the electron-phonon interaction. It is seen that, to within experimental error, the columns add properly, indicating internal consistency of analysis.

ACKNOWLEDGMENTS

The authors wish to thank R. Linz and M. Karamargin for help with the reduction of data, and H. Taylor for technical assistance. The computational part of this work was carried out via the facilities of the Computer Center of the University of Connecticut, which is supported by Grant No. GP-1819 of the National Science Foundation.

PHYSICAL REVIEW VOLUME 178, NUMBER 3 15 FEBRUARY 1969

Transport Equation for a Fermi Liquid in Random Scattering Centers. I. A Quasiparticle Description in the Macroscopic and Low-Temperature Limit*

JAMES L. SIGEL
Lincoln Laboratory,† Massachusetts Institute of Technology, Lexington, Massachusetts 02173
AND
PETROS N. ARGYRES‡
Lincoln Laboratory,† Massachusetts Institute of Technology, Lexington, Massachusetts
and
Northeastern University, Boston, Massachusetts 02115

(Received 12 September 1968)

The transport properties of an interacting fermion gas in the presence of randomly distributed scattering centers and a weak longitudinal force field are studied on the basis of a transport equation for the bare-particle distribution function. This equation, valid for arbitrary wavelength, frequency, and temperature, is derived by a generalization of a simple method due to Résibois. For the case of electrons, the transport equation is given in terms of the mean total electric field in the medium, thereby allowing a direct calculation of the transport coefficients of physical interest. The general theory is applied to the case of a slowly and smoothly varying driving field, low temperatures, and weak and dilute scattering centers. It is shown, up to second order in the interfermion interaction, that a transport equation for a quasiparticle distribution function can be derived. This equation has the form originally suggested by Landau with the interparticle and impurity scattering terms added. The connection between the bare-particle and the quasiparticle distribution functions is also obtained.

1. INTRODUCTION

THE linear electromagnetic properties of solids, such as metals and semiconductors, at low temperatures are determined to a large extent by the impurities in the crystal. Within the one-electron approximation, these properties are calculated on the basis of quantum transport equations, which have been derived by various authors.[1–5] All these theories neglect the electron-electron interaction and are, therefore, incapable of describing *a priori* such effects as the screening of the impurity potential, electron-electron scattering, and other more subtle many-body effects. Although the effects of the screening and the electron-electron scattering have at times been considered in various applications in a qualitative way, no convincing and self-contained theory has been given as yet even for these simple effects.

Recently progress has been made in the calculation of the transport properties of a degenerate, homogeneous, normal interacting electron gas in dilute random impurities. Langer[6] in a series of papers has been able

* Based in part on a thesis submitted by J. L. Sigel in partial fulfillment of the requirements of the degree of Doctor of Philosophy at the Massachusetts Institute of Technology.

† Operated with support from the U. S. Air Force.

‡ Permanent address: Physics Department, Northeastern University, Boston, Mass.

[1] W. Kohn and J. M. Luttinger, Phys. Rev. **108**, 590 (1957); **109**, 1892 (1958).

[2] D. A. Greenwood, Proc. Phys. Soc. (London) **71**, 585 (1958).

[3] K. Yamada, Progr. Theoret. Phys. (Kyoto) **28**, 299 (1962).

[4] C. V. Chester, Proc. Phys. Soc. (London) **81**, 938 (1963).

[5] P. N. Argyres and E. S. Kirkpatrick, Ann. Phys. (N. Y.) **42**, 513 (1967).

[6] J. S. Langer, Phys. Rev. **120**, 714 (1960); **124**, 1003 (1961); **127**, 5 (1962). See also remarks by P. C. Martin, *ibid.* **161**, 143 (1967).